Chemical Engineering Journal 236 (2014) 39–46

Contents lists available at ScienceDirect

Chemical Engineering Journal

journal homepage: www.elsevier.com/locate/cej

Synthesis, characterization, and dye sorption ability of carbon nanotube–biochar nanocomposites

Mandu Inyang [a], Bin Gao [a,*], Andrew Zimmerman [b], Ming Zhang [a], Hao Chen [a]

[a] Department of Agricultural and Biological Engineering, University of Florida, Gainesville, FL 32611, United States
[b] Department of Geological Sciences, University of Florida, Gainesville, FL 32611, United States

HIGHLIGHTS

- Hybrid multi-walled carbon nanotube (CNT)-coated biochars were synthesized.
- CNTs significantly enhanced the physiochemical properties of the biochars.
- CNT–biochar nanocomposites have good sorption ability to methylene blue.

ARTICLE INFO

Article history:
Received 6 August 2013
Received in revised form 16 September 2013
Accepted 18 September 2013
Available online 27 September 2013

Keywords:
Biochar
Carbon nanotubes
Sorption
Methylene blue
Dye
Nanocomposites

ABSTRACT

Innovative technologies incorporating engineered nanoparticles into biochar production systems could improve the functions of biochar for many applications including soil fertility enhancement, carbon sequestration and wastewater treatment. In this study, hybrid multi-walled carbon nanotube (CNT)-coated biochars were synthesized by dip-coating biomass in varying concentrations of carboxyl-functionalized CNT solutions (0.01% and 1% by weight) prior to slow pyrolysis. Untreated hickory and bagasse biochars (HC and BC, respectively) and CNT–biochar composites (HC–CNT and BC–CNT, respectively) were characterized, and the methylene blue (MB) sorption ability of the resulting chars was evaluated in batch sorption experiments. The addition of CNTs significantly enhanced the physiochemical properties of the biochars with HC–CNT-1% and BC–CNT-1% exhibiting the greatest thermal stabilities, surface areas (351 and 390 $m^2\ g^{-1}$, respectively), and pore volumes (0.14 and 0.22 cc g^{-1}, respectively). Sorption kinetic and isotherm data showed that, among the biochars examined, BC–CNT-1% had the highest MB sorption capacity (6.2 mg g^{-1}). While increased pH (up to ~7), promoted the uptake of MB by all the biochars, whether coated or not, increasing ionic strength decreased the uptake of MB by all biochars tested. These findings suggest that electrostatic attraction was the dominant mechanisms for the sorption of MB onto the chars, though diffusion controlled its rate. Hybridized CNT–biochar nanocomposite can thus be considered a promising, inexpensive sorbent material for removing dyes and organic pollutants from aqueous systems.

1. Introduction

The use and release of organic dyes in many industrial products are a threat to water systems [1]. The complex aromatic structure of dyes makes them of low biodegradability and stable toward light and chemical treatments [2]. Methylene blue (3,7-bis(dimethylamino)-phenothiain-5-ium chloride) is a cationic dye found in many industrial effluents that may induce aesthetic, and more importantly health problems such as cancers, reproductive and neurological disorders in humans and aquatic organisms [3]. A number of treatment techniques including ionic exchange, adsorption, coagulation, membrane filtration and photo-catalysis have been extensively tested for the removal of dyes from wastewater [4–8]. Among these methods, adsorption is known to be a more economical and simple treatment approach [2]. Thus, research on low-cost, high-capacity adsorbents for organic dyes is increasing [9].

Biochar is a low-cost, porous, carbon-rich product derived from the thermal degradation of organic matter (particularly waste biomass) in an oxygen-limited environment [10]. The benefits of employing eco-friendly biochars, including activated biochars, in wastewater treatment technologies have already been established [11–17]. In addition, a recent study showed that ENPs may bind to biochar surfaces (particularly after modification) to a greater extent than to commercial activated carbons [18]. Thus, marrying existing biochar technology with emerging nanotechnology to create hybrid nanomaterial-biochar composites, has great potential to

* Corresponding author. Tel.: +1 352 392 1864x285.
E-mail address: bg55@ufl.edu (B. Gao).

1385-8947/$ - see front matter © 2013 Elsevier B.V. All rights reserved.
http://dx.doi.org/10.1016/j.cej.2013.09.074

create a new class of environmentally-friendly and cost-effective sorbents to treat a wide array of contaminants [19–24].

Carbon nanotubes (CNTs) are cylindrical tubes of graphene material that exhibit exceptional properties such as ultra-low weight, high mechanical strength, and thermal and chemical stability [25]. The potential use of CNTs as adsorbents has generated much interest [2,26–29] because the hollow, layered structure of CNTs endows them with characteristically high specific surface areas and correspondingly high sorption capacities for various contaminants [26,30]. Moreover, chemically functionalized CNT surfaces, grafted with specific functional groups (carboxyl, hydroxyl, amine, fluorine) provide high-affinity sorption sites for increased binding of target pollutants such as dyes via electrostatic attractions or π–π electron bonding [9,31,32]. Despite these sorptive properties, practical application of CNTs remains limited by its poor solubility, and rapid aggregation in its native state [33]. Several research efforts have been made to overcome these limitations, by loading CNTs on sorptive supports using sol gel [34], crosslinking agents [35], and carbon vapor deposition (CVD) growth techniques [25,36]. However, the high cost and formation of by-products with many of these methods has made it necessary to consider other supports. Thus, biochar is examined here as such a potential, low-cost support for CNTs.

The overarching objective of this study was to develop a simple method to synthesize hybrid CNT–biochar nanocomposite material and test its potential applications. Our specific objectives were to: (1) characterize the CNT–biochar nanocomposite, (2) determine the effects of CNT hybridization on the physiochemical properties of the biochars, (3) examine the influence of pH, contact time, and ionic strength conditions on the sorption of MB on the CNT–biochar nanocomposite, and (4) elucidate and understand the interaction mechanisms governing the sorption of MB on the CNT–biochar nanocomposite.

2. Materials and methods

2.1. Materials

Carboxylic acid-functionalized multi-walled CNTs with diameters ranging 10–20 nm were purchased from the Sinonano Company (PR China). Hickory chips and sugarcane bagasse biomass were obtained from the North Florida Research and Education Center of the University of Florida. The biomass feedstocks were dried and milled to 500 μm size fraction. Methylene blue ($C_{16}H_{18}ClN_3S$, molecular weight, 319.86 g) and other chemicals employed in this study were of analytical grade and obtained from Fisher Scientific, Georgia.

2.2. Preparation of CNT–biochar nanocomposite

CNT suspensions were prepared by adding either 20 mg (0.01% by weight) or 2 g (1% by weight) of CNT powder to 200 ml of deionized (DI) water. The CNT suspensions were sonicated in an ultrasound homogenizer (Model 300 V/T, Biologics, Inc.) with an output frequency of 20 kHz for 1 h at pulse intervals of 12 min. The resulting suspensions were designated as CNT-0.01% and CNT-1%, respectively, and used for the preparation of CNT–biochar nanocomposite.

Milled hickory chips and sugarcane bagasse biomass (feedstocks) were converted to CNT–biochar nanocomposite following a dip-coating procedure [19,37]. Specifically, 10 g of each feedstock were placed in 100 ml of the CNT suspensions and stirred for 1 h using a magnetic stirrer at 500 rpm, after which, each of the dip-coated CNT treated feedstocks was removed and oven-dried at 105 °C. Next, each of the dried CNT-treated feedstocks was placed in a quartz tube, inside a tubular furnace (MTI, Richmond, CA) and pyrolyzed at 600 °C for 1 h at 10 °C/min in a flowing N_2 environment. In addition, each of the untreated feedstocks was also converted into the corresponding untreated biochar using the same pyrolysis conditions. The resulting biochars produced were designated as hickory chips (HC), CNT-modified hickory chips (HC–CNT-0.01% and HC–CNT-1%), sugarcane bagasse (BC), and CNT-modified sugarcane bagasse (BC–CNT-0.01% and BC–CNT-1%). All biochars were rinsed with distilled, de-ionized water several times, oven dried, and sealed in glass containers for subsequent testing.

2.3. Characterization

Elemental carbon, hydrogen, nitrogen and oxygen content (C, H, N, and O); zeta potential, pH, and surface areas of the sorbents were determined using previously reported methods [11,24]. Because all the sorbents were made at 600 °C, the volatile matter content was not determined. Thermogravimetric analysis (TGA) was performed in a stream of air at a heating rate of 10 °C/min with a Mettler TGA/DSC1 analyzer (Columbus, OH) to test the thermal stability of the samples. The morphology of CNT-modified biochar composites was examined by transmission electron microscopy (JEOL 2010F TEM). Physiochemical features of the samples were investigated by Raman spectroscopy (Renishaw Bio Raman).

2.4. Sorption of methylene blue

An initial evaluation of the sorption ability of the chars was conducted using MB solution in batch sorption experiments. About 25 mg of each test biochar was mixed in 50 ml digestion vessels (Environmental Express) with 12.5 ml of 20 mg L^{-1} MB solution at room temperature (22 ± 0.5 °C). The sample solutions and their corresponding blanks and experimental controls (without either sorbent or sorbate) were agitated for 24 h on a reciprocating shaker, then filtered through 0.22 μm pore size nylon membrane (GE cellulose nylon membranes). Measurements of MB concentrations in the filtrates were determined using a Thermo Scientific EVO 60 UV–VIS spectrophotometer at a wavelength of 665 nm. Sorbed amounts of MB on test biochars were calculated as the difference between the initial and final aqueous MB solution concentrations. Sorption experiments were conducted in duplicate and the average values are reported here.

Following the initial evaluation experiments, sorption kinetics and isotherm studies of MB sorption on unmodified biochar (HC and BC) and CNT–biochar nanocomposites (HC–CNT-1% and BC–CNT-1%) were conducted. To examine sorption kinetics, 25 mg of each sorbent was mixed with 12.5 ml of 20 mg L^{-1} MB solution in 50 ml digestion vessels at room temperature. The sample solutions and their corresponding controls were withdrawn from the agitator at time intervals of about 2 h up to 24 h and filtered through 0.22 μm pore size nylon membranes for measurements. The pH of the filtered sample solutions were noted prior to and after sorption experiments. Sorption isotherms were obtained by adding 25 mg of each biochar to 12.5 ml, MB solutions of varying concentrations (5–80 mg L^{-1}). Sorption kinetics and isotherm experiments were performed in triplicate and the average results are presented with standard deviations.

2.5. Effect of pH and ionic strength

The effect of pH on MB sorption by the CNT-modified and unmodified biochar sorbents was evaluated by adding 25 mg of each biochar to 12.5 ml of 20 mg L^{-1} MB solutions in 50 ml digestion vessels with pH condition ranging (2–10, adjusted by adding aqueous solutions of either 0.1 M NaOH or 0.1 mM HCl. To study the effect of ionic strength, pre-determined amounts of NaCl were

added to obtain 0.01 M, 0.05 M, 0.1 M, and 0.5 M ionic strength solutions. The sample mixtures and their corresponding blanks were agitated for 24 h, and then filtered and treated as described above. Sorption experiments at different pH or ionic strength were conducted in triplicate.

3. Results and discussion

3.1. Biochar properties

The properties of both hickory (HC) and bagasse biochars (BC) were generally improved by the addition of 1% CNTs (Table 1). In particular, the surface areas of HC–CNT-1% and BC–CNT-1% were about 3 and 40 times greater than their unmodified control biochars (HC and BC), surface areas , respectively, suggestion more CNTs were anchored to BC than to HC. In addition, the pore volume of the sorbents also increased with the addition of the CNTs (Table 1), suggesting the CNT pretreatment could potentially increase the porosity of the biochars. Results of the zeta potential measurements showed that the surfaces of the hybrid biochar sorbents also became increasingly negatively charged with increasing amounts of CNTs added, probably because the CNTs (zeta potential = −46.3 mv) used in this work are negatively charged.

TGA profiles of HC and BC samples exhibited a slightly higher thermal stability with increasing introduction of CNTs (Fig. 1a and b), though, the difference in stability was more obvious for BC–CNT nanocomposites. The thermal degradation of pyrolyzed carbon materials, typically show loss of moisture (50–100 °C), followed by the disappearance of transformation carbon (e.g., aromatic C═C groups) from 100 to 350 °C, and finally, the formation of graphitic chars beyond 350 °C [19,38]. Weight losses in both CNT-modified and unmodified biochars were insignificant until 350 °C, thereafter, comparatively greater weight losses (~80%) were observed in the unmodified chars from about 350–500 °C than CNT-modified chars (~70%). The thermal decomposition behavior of the CNT-1% biochars, particularly, BC–CNT-1% closely resembled the CNT thermal curve, degrading at about 400 °C.

Features of the Raman spectra (Fig. 2a and b) include the disorder mode D-band (~1350 cm^{-1}) induced by sp^3 hybridization and the tangential mode G-band, representing crystalline graphitic/sp^2 carbon stretching vibrations (1500–1600 cm^{-1}) [31,39]. Generally, the D-band originates from defects and functionalities (e.g., —OH, —C═O, —COOH, and —F) within CNT walls [40], and increased I_D/I_G indicates higher defect concentration (increased functional groups) on the sorbents surface [31]. Unmodified HC and BC biochars had lower I_D/I_G ratios (1.12 and 1.11 respectively), than CNT (1.78) (Table 1). But, after incorporating CNTs onto the biochars, I_D/I_G ratios of the hybrid HC–CNT and BC–CNT samples increased, indicating increased functionalities on the hybrid sorbents. TEM images of HC–CNT-1% and BC–CNT-1% (Supplementary information, Fig. S1) showed the presence of tubular CNT bundles (diameter, 15–25 nm) on the char surfaces which further demonstrates the incorporation of CNTs in the biochar nanocomposites.

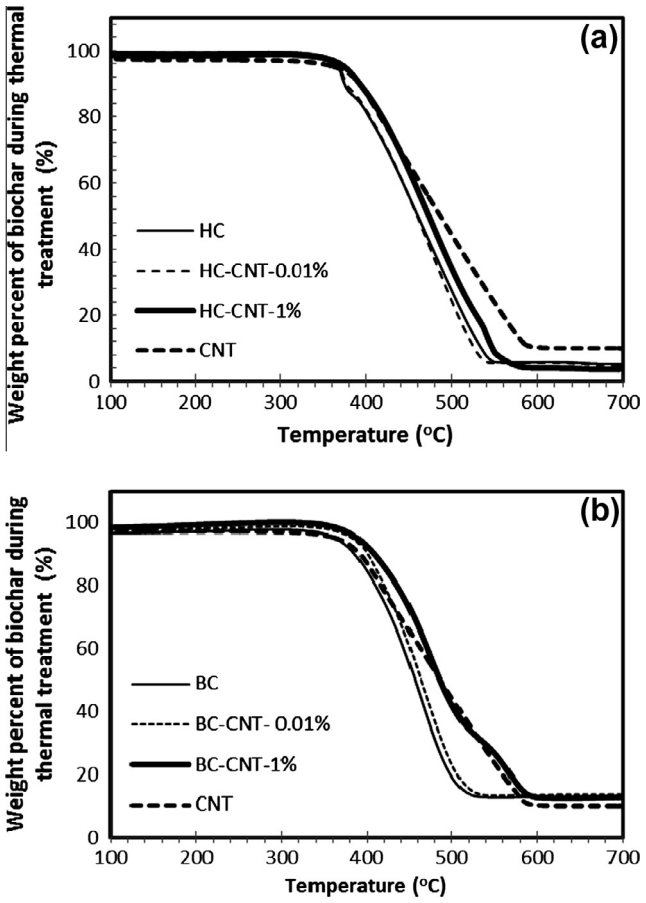

Fig. 1. Thermogravimetric analysis profiles biochar based sorbents: (a) HC and HC–CNT composites and (b) BC and BC–CNT composites.

3.2. Methylene blue removal efficiency of biochars

Though MB was sorbed by both CNT-modified and unmodified biochars, MB removal efficiencies increased with increasing CNT additions (Fig. 3). The highest removal of MB by the sorbents was observed for HC–CNT-1% (47% removal) and BC–CNT-1% (64% removal). The removal of MB by the biochars modified with 0.01% CNTs, however, was similar to or even slightly lower than that by the unmodified one (Fig. 3). These findings are consistent with characterization results which showed the most improvements in specific surface area/pore volume and surface chemistry properties (e.g., zeta potential and Raman functionality) of biochars with additions of 1% CNT. Several mechanisms have been proposed for the interaction of organic contaminants with pristine and functionalized CNT including hydrophobic interaction, hydrogen bonding, electrostatic attractions and π–π interactions between

Table 1
Structural and physiochemical properties of the biochar based sorbents.

Sample	pH	Zeta potential (mV)	BET N2 surface area ($m^2\ g^{-1}$)	Pore volume (cc g^{-1})	C %	H %	N %	O %	Raman intensity (disorder/order ratio) I_D/I_G
HC	7.3	−28.8	289	0.001	81.8	2.2	0.7	15.3	1.11
HC–CNT-0.01%	7.4	−33.2	257	0.003	84.1	2.5	0.4	13	1.14
HC–CNT-1%	7.5	−41.4	352	0.138	80.3	2.1	0.2	17.4	1.30
BC	6.9	−32.7	9	0.000	76.4	2.9	0.8	19.9	1.12
BC–CNT-0.01%	7.0	−34.1	120	0.008	79.3	2.2	0.8	17.7	1.15
BC–CNT-1%	7.3	−44.6	390	0.220	85.7	1.7	0.7	11.9	1.28

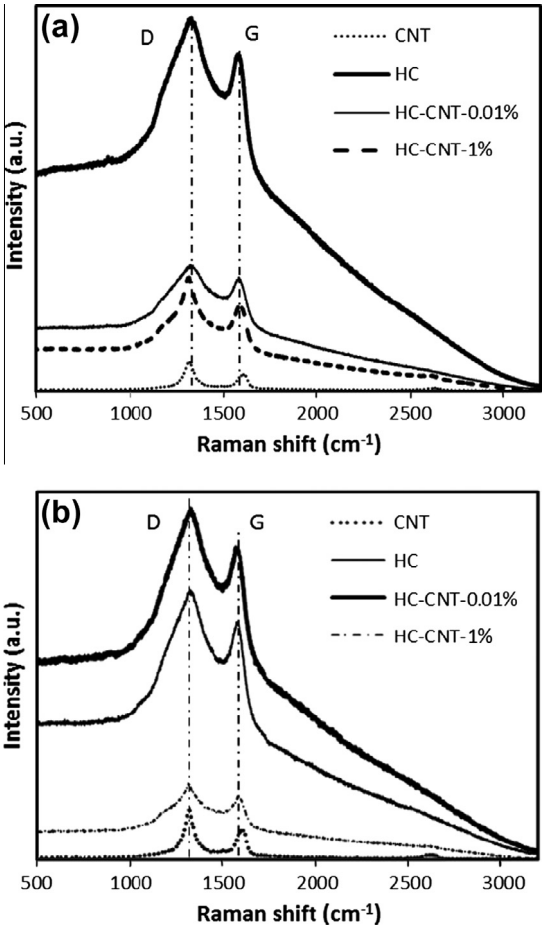

Fig. 2. Raman spectra of biochar based sorbents: (a) HC and HC–CNT composites and (b) BC and BC–CNT composites.

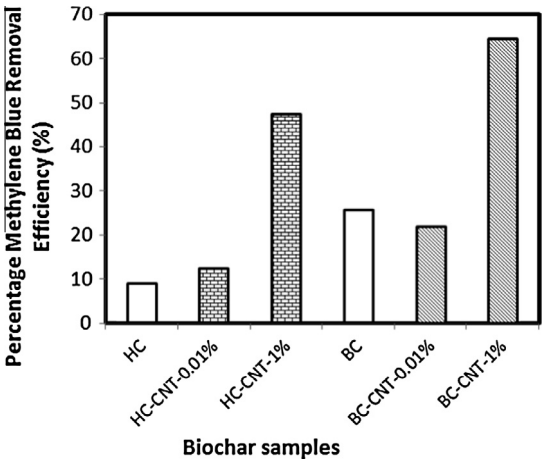

Fig. 3. Methylene blue removal efficiencies of biochar based sorbents.

graphitic surfaces of CNT and organic molecules containing C=C bonds [2,30,41]. To elucidate the sorption interaction between the hybrid-CNT-sorbents and MB, further testing under varied conditions was conducted using the HC–CNT-1% and BC–CNT-1%.

3.3. Sorption kinetics

Sorption versus time profiles for the sorbents showed different sorption behaviors for the biochars (Fig. 4a–d). For instance, pseudo-equilibrium times for MB sorption were reached in the order of BC–CNT-1% < HC < BC < HC–CNT-1%. The sorption kinetic data were simulated with the pseudo-first order, pseudo-second order, and Elovich models. The CNT–biochar nanocomposites exhibited much better correlation of the experimental data with first and second order models ($R^2 > 0.75$) than HC and BC ($R^2 < 0.59$, Table 2). The first (k_1) and second order (k_2) sorption rate constants were higher for HC (1.08 and 1.90 h^{-1}) and BC (18.94 and 19.44 h^{-1}) than for their respective CNT-modified chars (HC–CNT-1% (0.97 and 0.67 h^{-1}) and BC–CNT-1% (13.08 and 5.16 h^{-1})), suggesting faster initial uptake of MB on the unmodified biochars. This could be attributed to the fact that the CNT–biochar nanocomposites have larger porosities (pore volume), which could increase the diffusive interaction time to delay the initial MB sorption. Intraparticle diffusion kinetic plots were linear and well-correlated with MB sorption ($R^2 > 0.75$) for all sorbents (Supplementary information, Fig. S2), confirming the importance of the diffusive interaction between the MB and the sorbents.

The pseudo-second order model, which predominantly describes chemisorption processes and interaction of functional groups on sorbents with contaminants [42], was the best fit for BC–CNT-1% sorption kinetics data ($R^2 = 0.96$). This suggests stronger affiliations of MB to the —COOH functionality on BC–CNT-1% than present for the unmodified biochars. The Elovich model, which also evaluates chemisorption mechanisms [43], did very well modeling MB sorption by HC–CNT-1% ($R^2 = 0.98$) and may also due to the involvement of carboxyl groups in MB sorption.

3.4. Sorption isotherms

Equilibrium isotherms of HC, BC, HC–CNT-1%, and BC–CNT-1% (Fig. 5a–d) showed increasing uptake of MB with increasing concentrations of aqueous MB until apparent maximum sorption capacity was reached. Sorption capacities of HC–CNT-1% and BC–CNT-1%, indicated via Langmuir modeling (2.4 and 5.5 mg g^{-1}, respectively), were almost twice those of their respective unmodified biochar, (1.3 and 2.2 mg g^{-1}, respectively). Similar sorption capacities were reported for some carbonaceous waste materials but the observed values are much lower than those of some other hybrid CNT materials (Supplementary information, Table S1), suggesting further investigations are still need to optimize the synthesis of the CNT–biochar nanocomposites to improve their sorption capacities to MB.

While both Langmuir and Freundlich models reproduced the sorption isotherm data reasonably well, the Langmuir–Freundlich (L–F) model fit both unmodified and CNT-modified biochars ($R^2 > 0.90$) best (Table 2 and Fig. 5), indicating the sorption of MB on the biochar base sorbents could be controlled multiple mechanisms. In the literature, the L–F model is often used to describe the sorption of chemicals by heterogeneous materials, including biochars, through multiple processes [12,44]. In this work, the sorption of MB on the CNT–biochar nanocomposites could be controlled by two processes: (1) MB sorbed onto high affinity binding sites within CNT and (2) MB sorbs to biochar itself as the CNT sites become filled.

3.5. Effect of pH

Solution pH can influence both the surface charge of a sorbent as well as the degree of ionization and conformation of a sorbate (such as MB) [9,45,46]. With increasing pH, there was an increase in MB sorption by all the biochars, until pH of 7, above which, no significant pH dependence was observed (Fig. 6a). Similar trends have been reported in the literature for MB sorption on other sorbents [1,46]. All the biochars used in this study were predominantly negatively charged in DI water (Table 1), which

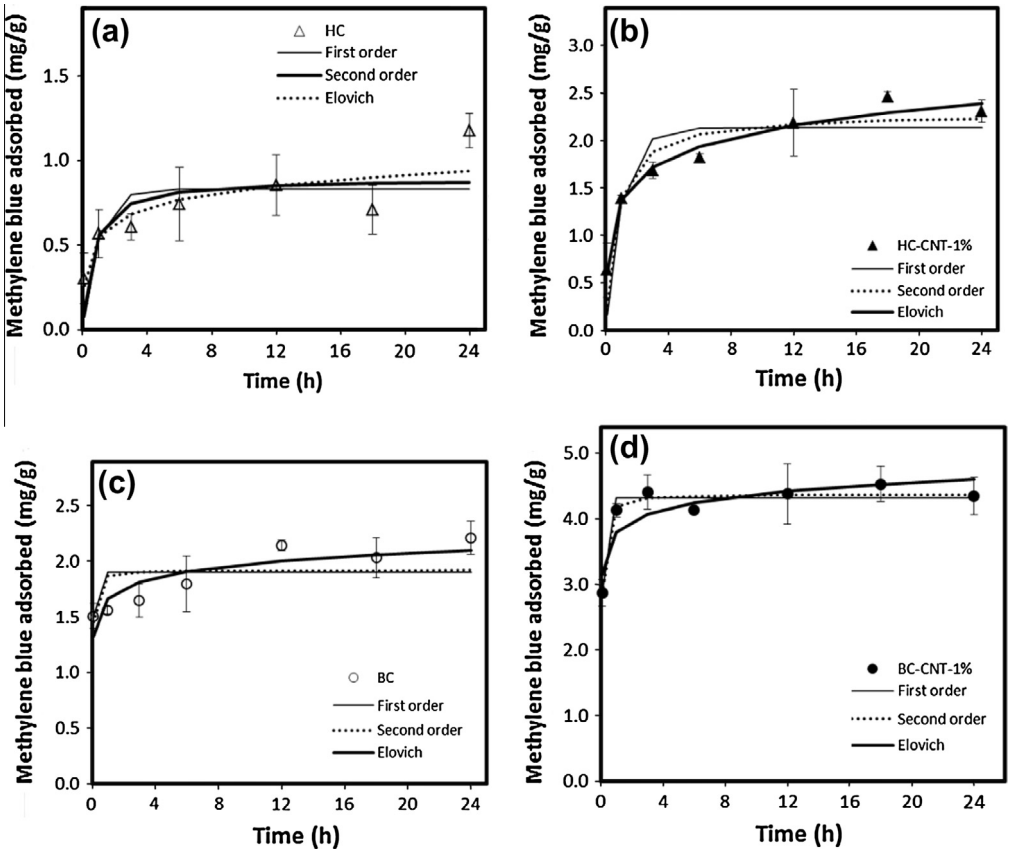

Fig. 4. Sorption kinetics plots of biochar based sorbents: (a) HC, (b) HC–CNT-1%, (c) BC, and (d) BC–CNT-1%.

Table 2
Summary of models and best-fit parameters of the sorption kinetics and isotherms.

Sorbents	Model*	Parameter 1	Parameter 2	Parameter 3	R^2
HC	First order ($q_t = q_e(1 - e^{-k_1 t})$)	k_1 = 1.08	q_{e1} = 0.80	–	0.464
	Second order $\left(q_t = \frac{k_2 q_e^2 t}{1+k_2 q_e^2 t}\right)$	k_2 = 1.90	q_{e2} = 0.89	–	0.588
	Elovich $\left(q_t = \frac{1}{\beta}\ln(\alpha\beta t + 1)\right)$	α = 10.86	β = 8.19	–	0.761
	Langmuir $\left(q_e = \frac{KS_{max}C_e}{1+KC_e}\right)$	K = 1.10	S_{max} = 1.28	–	0.930
	Freundlich ($q_e = K_f C_e^n$)	K_F = 0.62	n = 0.19	–	0.748
	Langmuir–Freundlich ($q_e = \frac{S_{max}(KC_e)^n}{1+(KC_e)^n}$)	K = 1.16	S_{max} = 1.24	n = 9.23	0.940
HC–CNT-1%	First order	k_1 = 0.97	q_{e1} = 2.10	–	0.759
	Second order	k_2 = 0.67	q_{e2} = 2.28	–	0.869
	Elovich	α = 22.2	β = 3.11	–	0.978
	Langmuir	K = 17.92	S_{max} = 2.40	–	0.851
	Freundlich	K_F = 1.44	n = 0.14	–	0.764
	Langmuir–Freundlich	K = 40.47	S_{max} = 2.40	n = 27.86	0.987
BC	First order	k_1 = 18.94	q_{e1} = 1.90	–	0.265
	Second order	k_2 = 19.44	q_{e2} = 1.92	–	0.336
	Elovich	α = 27107.52	β = 7.32	–	0.764
	Langmuir	K = 2.09	S_{max} = 2.20	–	0.917
	Freundlich	K_F = 1.07	n = 0.20	–	0.797
	Langmuir–Freundlich	K = 2.24	S_{max} = 2.20	n = 1.81	0.920
BC–CNT-1%	First order	k_1 = 13.08	q_{e1} = 4.30	–	0.935
	Second order	k_2 = 5.16	q_{e2} = 4.37	–	0.956
	Elovich	α = 699779.76	β = 3.91	–	0.799
	Langmuir	K = 4.84	S_{max} = 5.50	–	0.961
	Freundlich	K_F = 3.02	n = 0.18	–	0.757
	Langmuir–Freundlich	K = 5.12	S_{max} = 5.50	n = 1.08	0.961

* q_t and q_e are the amount of sorbate removed at time t and at equilibrium, respectively (mg g^{-1}), and k_1 and k_2 are the first-order and second-order sorption rate constants (h^{-1}), respectively, α is the initial sorption rate (mg g^{-1}) and β is the desorption constant (g mg^{-1}), K and K_f are the Langmuir bonding term related to interaction energies (L mg^{-1}) and the Freundlich affinity coefficient ($mg^{(1-n)}$ L^n g^{-1}), respectively, S_{max} is the Langmuir maximum capacity (mg g^{-1}), C_e is the equilibrium solution concentration (mg L^{-1}) of the sorbate, and n is the Freundlich linearity constant.

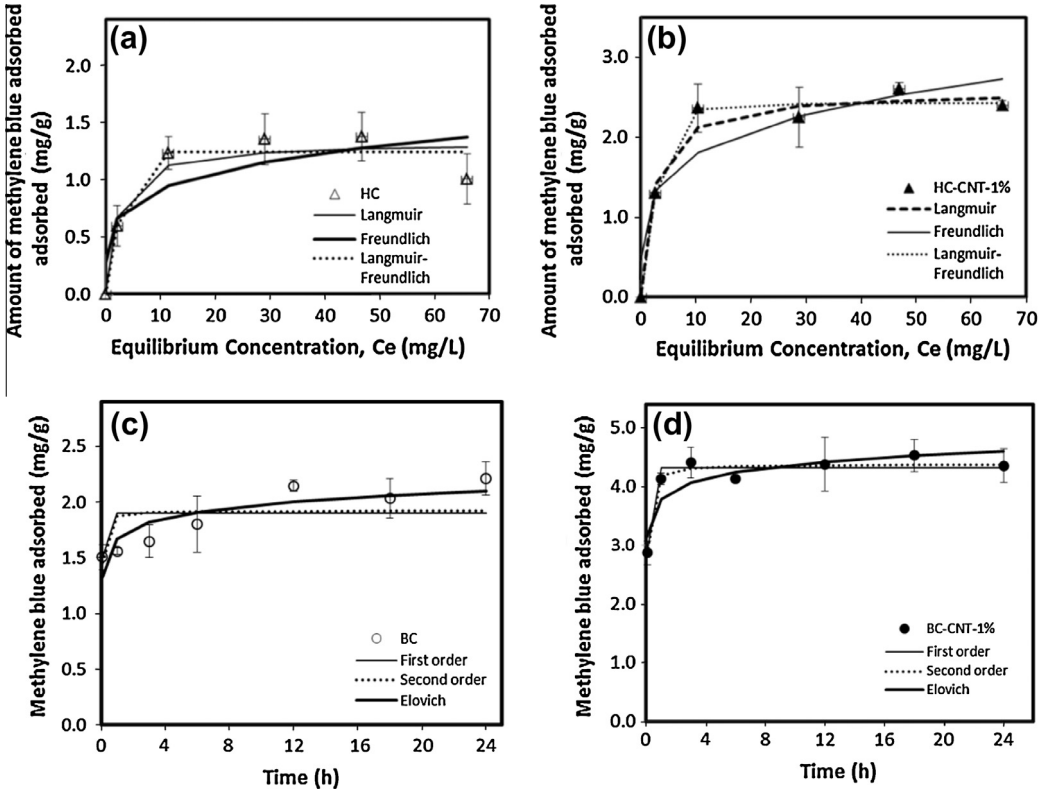

Fig. 5. Sorption isotherms of biochar based sorbents: (a) HC, (b) HC–CNT-1%, (c) BC, and (d) BC–CNT-1%.

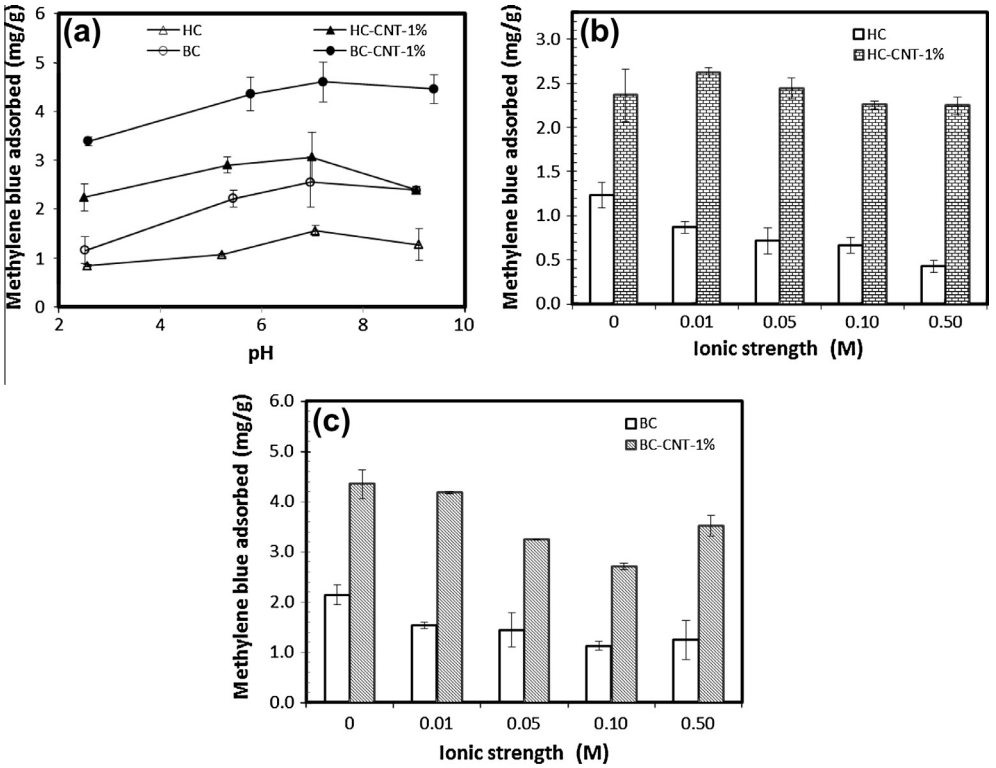

Fig. 6. Effects of solution chemistry on methylene sorption on biochar based sorbents: (a) pH effects, (b) ionic strength effects on HC and HC–CNT-1%, and (c) ionic strength effects on BC and BC–CNT-1%.

would promote the sorption of positively charged MB (pK_a 3.8) by electrostatic attraction [45]. In particular, the electrostatic attraction of positively charged MB to the CNT–biochar nanocomposites should increase with increasing pH (below 7) because of the increasing deprotonation of the functional (e.g., carboxyl and hydroxyl) groups of the CNTs within the biochar matrix. On the other

hand, because MB consists of benzene rings, which can donate π electrons to π-electron acceptors like the functional groups of the CNTs, π–π coupling may be another important mechanism promoting the sorption of MB on the CNT–biochar nanocomposites. In this case, a low pH causes protonation of the carboxyl groups, which should favor the sorption of strong π-donor compounds [1,47,48].

3.6. Effect of ionic strength

The presence of cations such as Na^+ have been shown previously to reduce the sorption of MB onto fungus [49]. In theory, when electrostatic forces between sorbent surfaces and sorbate ions are attractive, an increase in ionic strength will decrease the sorption capacity of the sorbate due to competition of Na^+ with positively charged MB for sorption sites [9]. Here, MB sorption onto all the biochar based sorbents decreased somewhat as concentrations of NaCl increased from 0.01 to 0.1 M (Fig. 6b and c), confirming involvement of electrostatic interaction in MB sorption. With 0.5 M of NaCl, however, there was no significant decrease, and even a slight increase in MB sorption by some of the sorbents. This effect has been reported previously and may arise from dimerization or aggregation of dye molecules at very high salt concentrations [9,50] and is independent of MB interactions with the sorbent.

4. Conclusions

Characterization of the sorbents indicated that the physiochemical properties (e.g., surface area, porosity, and thermal stability) of the biochars were enhanced by additions of CNTs. The BC–CNT-1% char had the highest sorption capacity to MB among all the sorbents, likely because it may have anchored more CNTs judging from its better thermal stability, higher surface area, and larger pore volume. The data collected suggests that electrostatic attraction was the dominant mechanism for sorption of MB onto the chars, but chemisorption such as pi–pi bonding should not be ruled out as a contributing sorption mechanism. Intrapore diffusion was also likely to control the rate at which MB was removed from solution onto the biochar based sorbents.

Though the overall sorption capacity of the CNT-hybridized chars studied were lower than those of some other hybrid sorbents reported in literature, the synthesis procedure employed here is simple, inexpensive, and can be further optimized. The results presented have established the potential of biochar-CNT hybrid sorbents to be used for environmental remediation of dyes and possibly other organic pollutants. In addition to their low cost, they may provide additional environmental benefits, such as carbon sequestration and soil amelioration.

Acknowledgment

This research was partially supported by the NSF through Grants: CBET-1054405 and CHE-1213333.

Appendix A. Supplementary material

Supplementary data associated with this article can be found, in the online version, at http://dx.doi.org/10.1016/j.cej.2013.09.074.

References

[1] U. Iriarte-Velasco, N. Chimeno-Alanis, M.P. Gonzalez-Marcos, J.I. Alvarez-Uriarte, Relationship between thermodynamic data and adsorption/desorption performance of acid and basic dyes onto activated carbons, J. Chem. Eng. Data 56 (2011) 2100–2109.
[2] L. Ai, J. Jiang, Removal of methylene blue from aqueous solution with self-assembled cylindrical graphene–carbon nanotube hybrid, Chem. Eng. J. 192 (2012) 156–163.
[3] H. Yan, W.X. Zhang, X.W. Kan, L. Dong, Z.W. Jiang, H.J. Li, H. Yang, R.S. Cheng, Sorption of methylene blue by carboxymethyl cellulose and reuse process in a secondary sorption, Colloid Surf. A 380 (2011) 143–151.
[4] S. Cheng, D.L. Oatley, P.M. Williams, C.J. Wright, Characterisation and application of a novel positively charged nanofiltration membrane for the treatment of textile industry wastewaters, Water Res. 46 (2012) 33–42.
[5] J. Ramkumar, S. Chandramouleeswaran, V. Sudarsan, R.K. Vatsa, S. Shobha, V.K. Shrikhande, G.P. Kothiyal, T. Mukherjee, Boroaluminosilicate glasses as ion exchange materials, J. Non-Cryst. Solids 356 (2010) 2813–2819.
[6] B.N. Lee, W.D. Liaw, J.C. Lou, Photocatalytic decolorization of methylene blue in aqueous TiO2 suspension, Environ. Eng. Sci. 16 (1999) 165–175.
[7] M. Malakootian, A. Fatehizadeh, Color removal from water by coagulation/caustic soda and lime, Iranian Journal of Environmental Health Science & Engineering 7 (2010) 267–272.
[8] N. Kannan, M.M. Sundaram, Kinetics and mechanism of removal of methylene blue by adsorption on various carbons – a comparative study, Dyes. Pigments 51 (2001) 25–40.
[9] J. Ma, F. Yu, L. Zhou, L. Jin, M.X. Yang, J.S. Luan, Y.H. Tang, H.B. Fan, Z.W. Yuan, J.H. Chen, Enhanced adsorptive removal of methyl orange and methylene blue from aqueous solution by alkali-activated multiwalled carbon nanotubes, ACS Appl. Mater. Interfaces 4 (2012) 5749–5760.
[10] J. Lehmann, A handful of carbon, Nature 447 (2007) 143–144.
[11] M. Inyang, B. Gao, Y. Yao, Y. Xue, A.R. Zimmerman, P. Pullammanappallil, X. Cao, Removal of heavy metals from aqueous solution by biochars derived from anaerobically digested biomass, Bioresour. Technol. 110 (2012) 50–56.
[12] G.N. Kasozi, A.R. Zimmerman, P. Nkedi-Kizza, B. Gao, Catechol and humic acid sorption onto a range of laboratory-produced black carbons (biochars), Environ. Sci. Technol. 44 (2010) 6189–6195.
[13] Y. Xue, B. Gao, Y. Yao, M. Inyang, M. Zhang, A.R. Zimmerman, K.S. Ro, Hydrogen peroxide modification enhances the ability of biochar (hydrochar) produced from hydrothermal carbonization of peanut hull to remove aqueous heavy metals: Batch and column tests, Chem. Eng. J. 200 (2012) 673–680.
[14] Y. Yao, B. Gao, M. Inyang, A.R. Zimmerman, X.D. Cao, P. Pullammanappallil, L.Y. Yang, Removal of phosphate from aqueous solution by biochar derived from anaerobically digested sugar beet tailings, J. Hazard. Mater. 190 (2011) 501–507.
[15] M. Zhang, B. Gao, Removal of arsenic, methylene blue, and phosphate by biochar/AlOOH nanocomposite, Chem. Eng. J. 226 (2013) 286–292.
[16] M.D. Inyang, B. Gao, W.C. Ding, P. Pullammanappallil, A.R. Zimmerman, X.D. Cao, Enhanced lead sorption by biochar derived from anaerobically digested sugarcane bagasse, Separ. Sci. Technol. 46 (2011) 1950–1956.
[17] P.R. Bonelli, M.E. Ramos, E.L. Buonomo, A.L. Cukierman, Potentialities of the biochar generated from raw and acid pre-treated sugarcane agricultural wastes, in: 8th Asia-Pacific International Symposium on Combustion and Energy Utilization Sochi, Russian Federation, 2006.
[18] M. Inyang, B. Gao, L. Wu, Y. Yao, M. Zhang, L. Liu, Filtration of engineered nanoparticles in carbon-based fixed bed columns, Chem. Eng. J. 220 (2013) 221–227.
[19] M. Zhang, B. Gao, Y. Yao, Y. Xue, M. Inyang, Synthesis, characterization, and environmental implications of graphene-coated biochar, Sci. Total. Environ. 435 (2012) 567–572.
[20] M. Zhang, B. Gao, S. Varnoosfaderani, A. Hebard, Y. Yao, M. Inyang, Preparation and characterization of a novel magnetic biochar for arsenic removal, Bioresour. Technol. 130 (2013) 457–462.
[21] M. Zhang, B. Gao, Y. Yao, Y.W. Xue, M. Inyang, Synthesis of porous MgO-biochar nanocomposites for removal of phosphate and nitrate from aqueous solutions, Chem. Eng. J. 210 (2012) 26–32.
[22] M. Zhang, B. Gao, Y. Yao, M. Inyang, Phosphate removal ability of biochar/MgAl-LDH ultra-fine composites prepared by liquid-phase deposition, Chemosphere 92 (2013) 1042–1047.
[23] Y. Yao, B. Gao, J. Chen, M. Zhang, M. Inyang, Y. Li, A. Alva, L. Yang, Engineered carbon (biochar) prepared by direct pyrolysis of mg-accumulated tomato tissues: Characterization and phosphate removal potential, Bioresour. Technol. 138 (2013) 8–13.
[24] Y. Yao, B. Gao, M. Inyang, A.R. Zimmerman, X. Cao, P. Pullammanappallil, L. Yang, Biochar derived from anaerobically digested sugar beet tailings: characterization and phosphate removal potential, Bioresour. Technol. 102 (2011) 6273–6278.
[25] J. Zhang, Z.-H. Huang, R. Lv, Q.-H. Yang, F. Kang, Effect of growing CNTs onto bamboo charcoals on adsorption of copper ions in aqueous solution, Langmuir 25 (2009) 269–274.
[26] Y. Tian, B. Gao, V.L. Morales, L. Wu, Y. Wang, R. Munoz-Carpena, C. Cao, Q. Huang, L. Yang, Methods of using carbon nanotubes as filter media to remove aqueous heavy metals, Chem. Eng. J. 210 (2012) 557–563.
[27] X.N. Li, H.M. Zhao, X. Quan, S.O. Chen, Y.B. Zhang, H.T. Yu, Adsorption of ionizable organic contaminants on multi-walled carbon nanotubes with different oxygen contents, J. Hazard. Mater. 186 (2011) 407–415.
[28] Y. Tian, B. Gao, H. Chen, Y. Wang, H. Li, Interactions between carbon nanotubes and sulfonamide antibiotics in aqueous solutions under various physicochemical conditions, J. Environ. Sci. Health Part a-Toxic/Hazard. Substances Environ. Eng. 48 (2013) 1136–1144.

[29] Y. Tian, B. Gao, V.L. Morales, H. Chen, Y. Wang, H. Li, Removal of sulfamethoxazole and sulfapyridine by carbon nanotubes in fixed-bed columns, Chemosphere 90 (2013) 2597–2605.
[30] X.M. Ma, M. Tsige, S. Uddin, S. Talapatra, Application of carbon nanotubes for removing organic contaminants from water, Mater. Express 1 (2011) 183–200.
[31] M. Theodore, M. Hosur, J. Thomas, S. Jeelani, Influence of functionalization on properties of MWCNT–epoxy nanocomposites, Mater. Sci. Eng. A-Struct. Mater. Prop. Microstruct. Process. 528 (2011) 1192–1200.
[32] S. Wang, Optimum degree of functionalization for carbon nanotubes, Curr. Appl. Phys. 9 (2009) 1146–1150.
[33] G.-W. Lee, J. Kim, J. Yoon, J.S. Bae, B.C. Shin, I.S. Kim, W. Oh, M. Ree, Structural characterization of carboxylated multi-walled carbon nanotubes, Thin Solid Films 516 (2008) 5781–5784.
[34] Z. Es'haghi, Z. Rezaeifar, G.H. Rounaghi, Z.A. Nezhadi, M.A. Golsefidi, Synthesis and application of a novel solid-phase microextraction adsorbent: hollow fiber supported carbon nanotube reinforced sol–gel for determination of phenobarbital, Anal. Chim. Acta 689 (2011) 122–128.
[35] K.L. Salipira, B.B. Mamba, R.W. Krause, T.J. Malefetse, S.H. Durbach, Cyclodextrin polyurethanes polymerised with carbon nanotubes for the removal of organic pollutants in water, Water SA 34 (2008) 113–118.
[36] Z.-H. Huang, F. Zhang, M.-X. Wang, R. Lv, F. Kang, Growth of carbon nanotubes on low-cost bamboo charcoal for Pb(II) removal from aqueous solution, Chem. Eng. J. 184 (2012) 193–197.
[37] D.T. Schoen, A.P. Schoen, L. Hu, H.S. Kim, S.C. Heilshorn, Y. Cui, High speed water sterilization using one-dimensional nanostructures, Nano Lett. 10 (2010) 3628–3632.
[38] B. Chen, D. Zhou, L. Zhu, Transitional adsorption and partition of nonpolar and polar aromatic contaminants by biochars of pine needles with different pyrolytic temperatures, Environ. Sci. Technol. 42 (2008) 5137–5143.
[39] H. Rong, K. Han, S. Li, Y. Tian, Muhuoyu, A novel method to graft carbon nanotube onto carbon fiber by the use of a binder, J. Appl. Polym. Sci. 127 (2013) 2033–2037.
[40] S. Osswald, E. Flahaut, H. Ye, Y. Gogotsi, Elimination of D-band in Raman spectra of double-wall carbon nanotubes by oxidation, Chem. Phys. Lett. 402 (2005) 422–427.
[41] A.K. Mishra, T. Arockiadoss, S. Ramaprabhu, Study of removal of azo dye by functionalized multi walled carbon nanotubes, Chem. Eng. J. 162 (2010) 1026–1034.
[42] C. Gerente, V.K.C. Lee, P. Le Cloirec, G. McKay, Application of chitosan for the removal of metals from wastewaters by adsorption – mechanisms and models review, Crit. Rev. Environ. Sci. Tech. 37 (2007) 41–127.
[43] S.H. Chien, W.R. Clayton, Application of Elovich equation to the kinetics of phosphate release and sorption in soils, Soil Sci. Soc. Am. J. 44 (1980) 265–268.
[44] G.P. Jeppu, T.P. Clement, A modified Langmuir–Freundlich isotherm model for simulating pH-dependent adsorption effects, J. Contam. Hydrol. 129 (2012) 46–53.
[45] S.I.L.P. Dias, S.T. Fujiwara, Y. Gushikem, R.E. Bruns, Methylene blue immobilized on cellulose surfaces modified with titanium dioxide and titanium phosphate: factorial design optimization of redox properties, J. Electroanal. Chem. 531 (2002) 141–146.
[46] F.A. Pavan, E.C. Lima, S.L.P. Dias, A.C. Mazzocato, Methylene blue biosorption from aqueous solutions by yellow passion fruit waste, J. Hazard. Mater. 150 (2008) 703–712.
[47] L. Ji, W. Chen, S. Zheng, Z. Xu, D. Zhu, Adsorption of sulfonamide antibiotics to multiwalled carbon nanotubes, Langmuir 25 (2009) 11608–11613.
[48] D.Q. Zhu, S.H. Hyun, J.J. Pignatello, L.S. Lee, Evidence for pi–pi electron donor–acceptor interactions between pi-donor aromatic compounds and pi-acceptor sites in soil organic matter through pH effects on sorption, Environ. Sci. Technol. 38 (2004) 4361–4368.
[49] N.S. Maurya, A.K. Mittal, P. Cornel, E. Rother, Biosorption of dyes using dead macro fungi: effect of dye structure, ionic strength and pH, Bioresour. Technol. 97 (2006) 512–521.
[50] P. Mukerjee, A.K. Ghosh, Thermodynamic aspects of the self-association and hydrophobic bonding of methylene blue. Model system for stacking interactions, J. Am. Chem. Soc. 92 (1970) 6419–6424.